

Conformational Fluctuations and Electronic Properties in Myoglobin

MASSIMILIANO ASCHI,¹ COSTANTINO ZAZZA,² RICCARDO SPEZIA,³ CECILIA BOSSA,³
ALFREDO DI NOLA,³ MAURIZIO PACI,⁴ ANDREA AMADEI⁴

¹*Dipartimento di Chimica, Ingegneria Chimica e Materiali Università degli studi via Vetoio,
67010, L'Aquila, Italy*

²*CASPUR, Supercomputing Center for University and Research, via dei Tizii 6b,
00185 Roma, Italy*

³*Dipartimento di Chimica, Università di Roma "La Sapienza" P.le Aldo Moro 5,
00185 Roma, Italy*

⁴*Dipartimento di Scienze e Tecnologie Chimiche Università di Roma "Tor Vergata" via della
Ricerca Scientifica 1 I-00133 Roma, Italy*

Received 7 October 2003; Accepted 2 December 2003

Abstract: In this article we use the recently developed perturbed matrix method (PMM) to investigate the effect of conformational fluctuations on the electronic properties of heme in Myoglobin. This widely studied biomolecule has been chosen as a benchmark for evaluating the accuracy of PMM in a large and complex system. Using a long, 80-ns, molecular dynamics simulation and unperturbed Configuration Interaction (CISD) calculations in PMM, we reproduced the main spectroscopic features of deoxy-Myoglobin. Moreover, in line with our previous results on a photosensitive protein, this study reveals a clear dynamical coupling between electronic properties and conformational fluctuations, suggesting that this correlation could be a general feature of proteins.

© 2004 Wiley Periodicals, Inc. J Comput Chem 25: 974–984, 2004

Key words: conformational fluctuations; electronic properties; Myoglobin; perturbed matrix method

Introduction

Understanding the relationship between the conformational fluctuations and the biological function of a protein is a longstanding and fascinating problem in molecular biology. In this context, particularly in the last 2 decades, a large amount of information has been provided by theoretical and computational methodologies such as classical molecular dynamics (MD) and Monte Carlo (MC) simulations.^{1–5} Nevertheless, despite the important advances, many questions remain still open, mainly for the intrinsic limitations of the classical view of the molecules. In particular, of great interest is the question as to whether and to what extent the conformational fluctuations of a protein affect the electronic properties of its active site. An answer to the above question would represent a fundamental breakthrough in the comprehension, at the atomic level, of some crucial biochemical and biophysical processes ranging from the spectroscopic behavior of a chromophore into the active site, to the mechanism of an enzymatic reaction. Actually, many aspects related to the electronic degrees of freedom of different biologically relevant systems have been repeatedly addressed in the last years using different quantum-mechanical

(QM) and mixed quantum-mechanical molecular-mechanics (QM/MM) approaches.^{6–9} However, the evaluation of the coupling of the electronic degrees of freedom with the motion of the overall protein is a less investigated aspect.¹⁰ In this context, we have recently proposed^{11,12} a method, the Perturbed Matrix Method (PMM), which has, as a peculiar feature, the capability of merging, through the very first principles of the quantum mechanics, the unperturbed electronic properties of a portion of the biological system with the classical molecular dynamics simulation of the surrounding protein acting as a perturbing field. This method has been recently applied successfully to a model system provided by a light-harvesting Peridinin–Chlorophyll–Protein of *Amphidinium carterae*.¹³ From this study an interesting correlation between the protein conformational fluctuations and the electronic properties of the chlorophyll has emerged. More precisely, the large concerted

Correspondence to: M. Aschi; e-mail: aschi@caspur.it

Contract/grant sponsor: MURST 2001 PRIN (Structural Biology and Dynamics of Redox Proteins).

Contract/grant sponsor: Centro di eccellenza (BEMM), University of Rome (La Sapienza; to A. Di Nola).

motions of the protein, even at a relatively large distance from the reaction center and taking place on a relatively large time scale, appear to sharply modulate the ground to first excited state energy gap of the chromophore providing a new and stimulating view of the relationship between the structure and the chemical determinants, which are the basis of protein function. On the basis of these findings we decided to investigate, with the same strategy, the spectroscopic features of another important biological system: the Myoglobin (Mb). Mb is a monomeric protein that transports molecular oxygen from hemoglobin to the terminal mitochondrial oxidase in muscle. This function is carried out by reversibly binding the oxygen at the ferrous heme covalently bound to the protein at the proximal histidine. This biologically relevant protein has been extensively studied both theoretically^{1,14,15} and experimentally.^{16–19} In this work we have focussed our attention in particular on the deoxy form of Mb, hereafter termed as deoxy Mb. The UV-Vis spectroscopic behavior of Mb in aqueous solution at room temperature both in the oxy and deoxy form is very well characterized.^{20,21} In particular, in addition to the π - π^* porphyrin absorption, i.e., the strong Soret band at 435 nm and the weak Q band at 560 nm, the deoxy form shows additional bands such as the porphyrin-iron charge transfer at 763 nm and the d - π^* iron-porphyrin charge transfer beyond 900 nm. In this article, by means of a further application of our PMM methodology we will focus our attention in trying to reproduce the above UV-Vis spectra with the precise aim of elucidating the effect of the overall protein conformational fluctuations on the transition energies and moments of deoxy Mb. A correct interpretation of such an effect could be a further step in the direction of understanding the actual role of protein structure and dynamics in biological activity.

Methods

In the first step of the present study we carried out a detailed investigation on the structural and dynamical features of the deoxy Mb. For this purpose we performed classical molecular dynamics (MD) simulations of the above protein starting from the corresponding crystal structure.²² The molecule was put into a cubic box at a distance larger than 0.7 nm from the walls. The box was then filled with water molecules described by the single-point charge model.²³ Water molecules were initially minimized using the steepest descent procedure followed by 20 ps of MD run with geometrical constraints applied to the protein. The overall system was then slowly heated from 50 to 300 K, and a simulation of 80 ns was finally carried out in the NVT ensemble. The temperature was kept constant by the isogaussian algorithm.²⁴ Periodic boundary conditions were systematically applied and long-range interactions were treated using the Particle-Mesh Ewald method.²⁵ The algorithm LINCS²⁶ was used to constrain bond lengths, and the roto-translational constraints²⁷ were also adopted in the simulation. Finally, to speed up the calculation, an integration time step of 4 fs was employed, using the Dummy Atoms technique.²⁸ At this purpose we have redistributed the water oxygen mass on the hydrogen atoms to improve the stability of the simulation. In the above run the GROMACS package was used for obtaining the trajectory. The same program and a certain number of our own routines, were adopted for analyzing the trajectory. In the second

step of the investigation we addressed the study of the unperturbed electronic properties of the heme. For this purpose we selected, as a portion of the system to be explicitly treated quantum mechanically, the complex iron-porphyrin-imidazole in its average structure extracted from 80 ns of simulation. Single-structure calculations are justified by the extremely low flexibility shown by such a complex along the simulation (*vide infra*). Both the singlet, triplet, and quintet states were evaluated. For the latter one, which from experimental evidences turned out to be the ground state of deoxy Mb, we evaluated the ground and the first eight excited states. These calculations were carried out at the CISD level of theory²⁹ using an active space containing 14 electrons in 16 orbitals. In this method the different configurations are generated by singly and doubly exciting the active electrons. Both the restricted and unrestricted formalism was adopted in conjunction with two different basis sets. The Triple Zeta function by Ahlrichs³⁰ was used for the iron, whereas the minimal STO-3G³¹ for all the remaining atoms. The choice of the above level of theory was essentially driven by two factors: first, the dimension of the system did not allow the application of a more accurate level of theory; second, the results provided by the above basis set turned out to reproduce the results found in the literature.^{32–34} In the final step of the work we evaluated, through the application of the PMM procedure described in the Theory section, the ground to excited-states energy gap with the precise aim of evaluating, by also calculating the corresponding transition dipoles, the related spectroscopical signal. All the quantum chemical calculations for the unperturbed eigenstates were performed using the Gamess US package.³⁵

Theory

The time-independent Schroedinger's equation, in matrix notation, for a perturbed system is

$$\tilde{H}c_i = \mathcal{U}_i c_i \quad (1)$$

where $\tilde{H} = \tilde{H}^0 + \tilde{V}$, c_i is the i th eigenvector of the perturbed Hamiltonian matrix \tilde{H} , \mathcal{U}_i the corresponding Hamiltonian eigenvalue, \tilde{H}^0 is the unperturbed Hamiltonian matrix and \tilde{V} is the perturbation energy matrix. The Hamiltonian matrix and its eigenvectors can be expressed in the basis set defined by the unperturbed Hamiltonian matrix eigenvectors, and hence, the element of the Hamiltonian matrix is

$$H_{i,i'} = \langle \Phi_i^0 | \hat{H} | \Phi_{i'}^0 \rangle = \mathcal{U}_i^0 \delta_{i,i'} + \langle \Phi_i^0 | \hat{V} | \Phi_{i'}^0 \rangle \quad (2)$$

where Φ_i^0 is the i th eigenfunction of the unperturbed Hamiltonian operator, \mathcal{U}_i^0 the corresponding energy eigenvalue, $\delta_{i,i'}$ the Kronecker's delta and \hat{V} the perturbation energy operator. From the above equations it is evident that for obtaining the perturbed eigenvectors and eigenvalues, and hence every property of the perturbed Hamiltonian eigenstates, we only have to diagonalize the matrix \tilde{H} , as given by eq. (2). For a system interacting with an external electric field, we can express in general the perturbation operator in eq. (2) in terms of the electric potential \mathcal{V} as

$$\hat{V} = \sum_j q_j \mathcal{V}(\mathbf{r}_j) \quad (3)$$

with \mathbf{r}_j the coordinates of the j th charged particle and q_j the corresponding charge. Expanding \mathcal{V} around a given position \mathbf{r}_0 we have

$$\begin{aligned} \mathcal{V}(\mathbf{r}_j) &\cong \mathcal{V}(\mathbf{r}_0) - \sum_{k=1}^3 E_k (r_{j,k} - r_{0,k}) \\ &- \frac{1}{2} \sum_{k'=1}^3 \sum_{k=1}^3 \left(\frac{\partial E_k}{\partial r_{k'}} \right)_{\mathbf{r}=\mathbf{r}_0} (r_{j,k} - r_{0,k})(r_{j,k'} - r_{0,k'}) + \dots \\ E_k &= - \left(\frac{\partial \mathcal{V}}{\partial r_{j,k}} \right)_{\mathbf{r}_j=\mathbf{r}_0} = - \left(\frac{\partial \mathcal{V}}{\partial r_k} \right)_{\mathbf{r}=\mathbf{r}_0} \end{aligned}$$

where k and k' define the three components of a vector in space and \mathbf{r} is the generic position vector. From these equations, defining with q_T the total charge, we readily obtain

$$\langle \Phi_i^0 | \hat{V} | \Phi_i^0 \rangle \cong q_T \mathcal{V}(\mathbf{r}_0) \delta_{i,i'} - \mathbf{E} \cdot \langle \Phi_i^0 | \hat{\boldsymbol{\mu}} | \Phi_i^0 \rangle + \frac{1}{2} \text{Tr}[\hat{\Theta} \tilde{Q}_{i,i'}] + \dots \quad (4)$$

$$Q_{k,k'}^{i,i'} = [\tilde{Q}_{i,i'}]_{k,k'} = \sum_j q_j \langle \Phi_i^0 | (r_{j,k} - r_{0,k})(r_{j,k'} - r_{0,k'}) | \Phi_i^0 \rangle \quad (5)$$

where

$$\Theta_{k,k'} = - \left(\frac{\partial E_k}{\partial r_{k'}} \right)_{\mathbf{r}=\mathbf{r}_0} \quad (6)$$

$$\hat{\boldsymbol{\mu}} = \sum_j q_j (\mathbf{r}_j - \mathbf{r}_0) \quad (7)$$

Hence, the complete perturbed Hamiltonian matrix is

$$\hat{H} \cong \hat{H}^0 + \hat{I} q_T \mathcal{V}(\mathbf{r}_0) + \hat{Z}_1(\mathbf{E}) + \hat{Z}_2(\hat{\Theta}) + \dots \quad (8)$$

$$[\hat{Z}_1]_{i,i'} = -\mathbf{E} \cdot \langle \Phi_i^0 | \hat{\boldsymbol{\mu}} | \Phi_i^0 \rangle \quad (9)$$

$$[\hat{Z}_2]_{i,i'} = \frac{1}{2} \text{Tr}[\hat{\Theta} \tilde{Q}_{i,i'}] \quad (10)$$

From the last equations it is evident that a second-order expansion of the electric potential, able to describe electric fields up to linear behavior over the molecular size, requires the knowledge of the total charge and the unperturbed dipoles and quadrupoles. Higher order expansions can, in principle, be used, but would require information on higher order multipoles that are typically very difficult to obtain. Moreover, it is rather unusual that an applied electric field is beyond the linear approximation over a molecular size, at least neglecting local atomic interactions typically described by short-range potentials such as the Lennard–Jones one.

A few considerations and assumptions are now necessary: (a) we consider Born–Oppenheimer (BO) surfaces; (b) we assume terms from quadrupoles on as very small and able to provide only local atomic (short range) interactions; and (c) we consider only the first vertical electronic excitations;

Hence, defining with \mathbf{r}_n the nuclear coordinates of the quantum center and with \mathbf{x} the coordinates of the atoms providing the (classical) perturbing field we can write

$$\hat{H}(\mathbf{r}_n, \mathbf{x}) \cong \hat{H}^0(\mathbf{r}_n) + q_T \mathcal{V}(\mathbf{r}_0, \mathbf{x}) \hat{I} + \hat{Z}_1(\mathbf{E}(\mathbf{x}), \mathbf{r}_n) + \Delta V(\mathbf{r}_n, \mathbf{x}) \hat{I} \quad (11)$$

where $\Delta V(\mathbf{r}_n, \mathbf{x})$ approximates the perturbation due to all the terms from the quadrupoles on, as a simple short range potential. Hence, the perturbed BO Hamiltonian eigenvalues ε_i are, within this approximation,

$$\varepsilon_i = \varepsilon_i' + q_T \mathcal{V}(\mathbf{r}_0, \mathbf{x}) + \Delta V(\mathbf{r}_n, \mathbf{x}) \quad (12)$$

where

$$(\hat{H}^0 + \hat{Z}_1) \mathbf{c}_i = \varepsilon_i' \mathbf{c}_i \quad (13)$$

and \mathbf{c}_i is the i th perturbed eigenvector. We then have $\varepsilon_i - \varepsilon_0 = \varepsilon_i' - \varepsilon_0'$, which has been used for the calculation of the excitation energy. Note that from the set \mathbf{c}_i we can, in principle, obtain any possible perturbed property, for example, the perturbed transition dipole $\boldsymbol{\mu}_{i,j} = \langle \Phi_i | \hat{\boldsymbol{\mu}} | \Phi_j \rangle$ is

$$\boldsymbol{\mu}_{i,j} = \mathbf{c}_i^{*T} \Lambda_x^0 \mathbf{c}_j + \mathbf{c}_i^{*T} \Lambda_y^0 \mathbf{c}_j + \mathbf{c}_i^{*T} \Lambda_z^0 \mathbf{c}_j \quad (14)$$

$$[\Lambda_x^0]_{i,i'} = \langle \Phi_i^0 | \hat{\mu}_x | \Phi_i^0 \rangle \quad (15)$$

$$[\Lambda_y^0]_{i,i'} = \langle \Phi_i^0 | \hat{\mu}_y | \Phi_i^0 \rangle \quad (16)$$

$$[\Lambda_z^0]_{i,i'} = \langle \Phi_i^0 | \hat{\mu}_z | \Phi_i^0 \rangle \quad (17)$$

where obviously Φ is the perturbed Hamiltonian eigenfunction and \mathbf{c}^{*T} is the transpose of the complex conjugated of \mathbf{c} (typically from quantum chemical calculations \hat{H} has only real elements and, hence, $\mathbf{c} = \mathbf{c}^*$ is a real eigenvector).

We can also express the free energy change for an electronic excitation of the quantum center, with all the environment molecules in their electronic ground states as

$$\Delta A = -kT \ln \left[\frac{\int e^{-\beta \mathcal{U}_i} d\xi d\mathbf{x} d\boldsymbol{\pi}_\xi d\boldsymbol{\pi}_x}{\int e^{-\beta \mathcal{U}_0} d\xi d\mathbf{x} d\boldsymbol{\pi}_\xi d\boldsymbol{\pi}_x} \right] = -kT \ln \langle e^{-\beta(\mathcal{U}_i - \mathcal{U}_0)} \rangle_{\mathcal{U}_0} \quad (18)$$

$$\langle e^{-\beta(\mathcal{U}_i - \mathcal{U}_0)} \rangle_{\mathcal{U}_0} = \frac{\int e^{-\beta(\mathcal{U}_i - \mathcal{U}_0)} e^{-\beta \mathcal{U}_0} d\xi d\mathbf{x} d\boldsymbol{\pi}_\xi d\boldsymbol{\pi}_x}{\int e^{-\beta \mathcal{U}_0} d\xi d\mathbf{x} d\boldsymbol{\pi}_\xi d\boldsymbol{\pi}_x}$$

$$\mathcal{U}_i = \varepsilon_i + \mathcal{K}_\xi + \mathcal{U}_{env,i}$$

where ξ are the classical nuclear degrees of freedom of the quantum center, $\boldsymbol{\pi}$ the conjugated momenta, \mathcal{K}_ξ the (classical) kinetic energy of the quantum center and $\mathcal{U}_{env,i}$ the internal energy of the

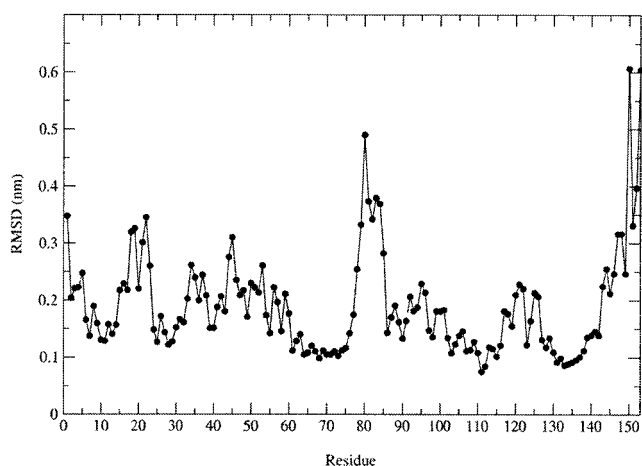


Figure 1. Root-mean-square deviation from crystal structure of C_{α} atoms. The values are averaged over the three spatial components.

environment (excluding the interaction with the quantum center) obtained when the quantum center is in the i th electronic state and all the environment molecules are in their electronic ground states. Note that in the case the environment energy is basically independent of the electronic state of the quantum center, as we assume neglecting atomic polarization, then ${}^0u_i - {}^0u_0 = \varepsilon'_i - \varepsilon'_0$. This last equation has been used for the calculation of the excitation free energy.

Results and Discussion

Molecular Dynamics Simulation

In the first part of our investigation we focus our attention on the structural and dynamical features of deoxy Mb in aqueous solution as provided by the 80-ns MD simulation. In this article we will only remark the essential aspects of the MD simulations of the deoxy Mb.

The time course of the root-mean-square deviation (RMSD) of the C_{α} atoms with respect to the crystal structure shows that within 5 ns a stable RMSD is reached, indicating that the system is equilibrated. The analysis of the RMSD for each residue of the backbone, reported in Figure 1, shows that the largest deviation from the crystal structure is present in correspondence of the loop EF and the N- and C-terminus. As already remarked in the Methods section, a necessary condition that allows the use of single-structure unperturbed basis set in the PMM calculations, is the rigidity of the quantum center. As reported in Figure 2, the heme reveals basically a rigid structure with the only exception of the two propionate groups, i.e., atoms 14–17 and 44–47, which, on the other hand, sharply fluctuate. For this reason the above groups were disregarded from the definition of the quantum center (*vide infra*). Finally, to characterize in details the large amplitude motions of the deoxy Mb, the essential dynamics analysis³⁶ was carried out on the equilibrated portion of the trajectory. This principal component procedure allows to separate the intramolec-

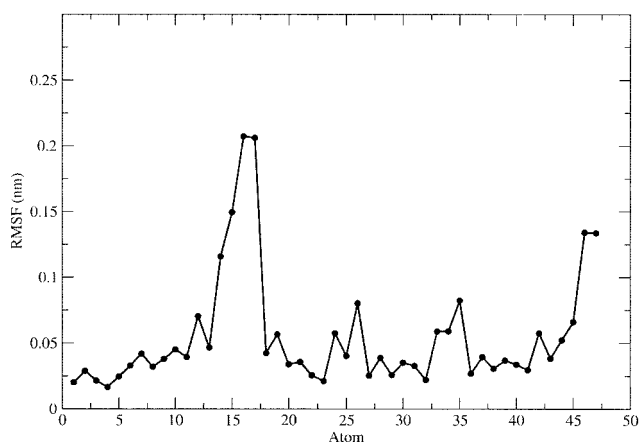


Figure 2. Root-mean-square fluctuations of heme atoms. The values are averaged over the three spatial components.

ular large collective motions (essential motions) from the remaining small amplitude fluctuations (near constrained motions). In fact, by diagonalizing the covariance matrix of the atomic positional fluctuations we obtain a set of generalized coordinates corresponding to the eigenvectors of the matrix. Each eigenvector represents the direction in configurational space associated with the largest fluctuation (eigenvalue) in the space defined by the eigenvector considered and the others with smaller eigenvalues. Hence, from the diagonalization of the C_{α} covariance matrix we characterized the deoxy Mb dynamics. The cumulative (normalized) fluctuations, i.e., sum of eigenvalues, of the first 50 eigenvectors is reported in Figure 3 with the corresponding eigenvalues. From such a figure it is possible to assess that the first 10 eigenvectors, i.e., the most important collective motions accounting for 75% of the total fluctuations, can be used to define the essential subspace. From the same figure it is also clear that within

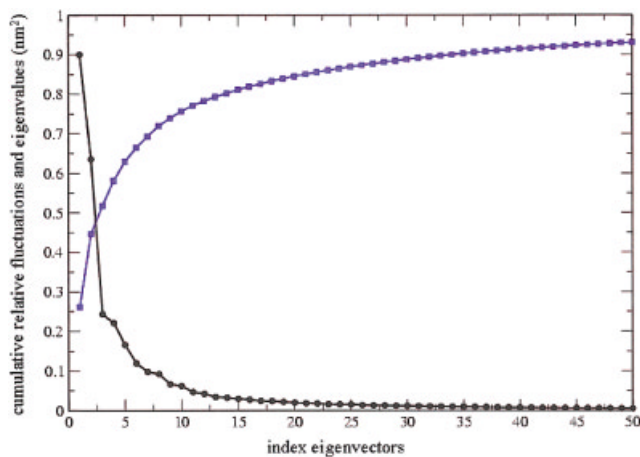


Figure 3. C_{α} eigenvalues (circles) and normalized cumulative fluctuation (squares) as obtained from MD simulation of Myoglobin. [Color figure can be viewed in the online issue, which is available at <http://www.interscience.wiley.com>]

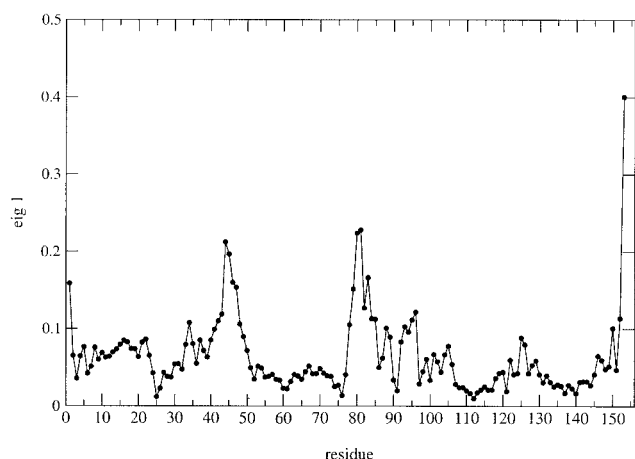


Figure 4. Components of the first C_α eigenvector.

this essential subspace the first two eigenvectors represent by far the dominant internal motions. For this reason their feature has been reported in more details by showing, in Figures 4 and 5, their components. From such figures it clearly emerges that loops provide the largest contribution to the internal motions of Mb. This latter result can be better appreciated by observing Figure 6a and b where we report the superposition of 10 configurations obtained by considering C-alpha motions only due to the first and second eigenvectors.

Quantum Chemical Calculations

We evaluated the unperturbed wave functions of the quantum center, defined as the portion of the overall system whose electronic degrees of freedom should be explicitly taken into account. From the previous MD analysis we found that a good candidate for the evaluation of the unperturbed basis set is the imidazole-iron(II)-porphyrin complex, hereafter indicated as FeP(Im), showing the average structure reported in Figure 7. On this structure, we

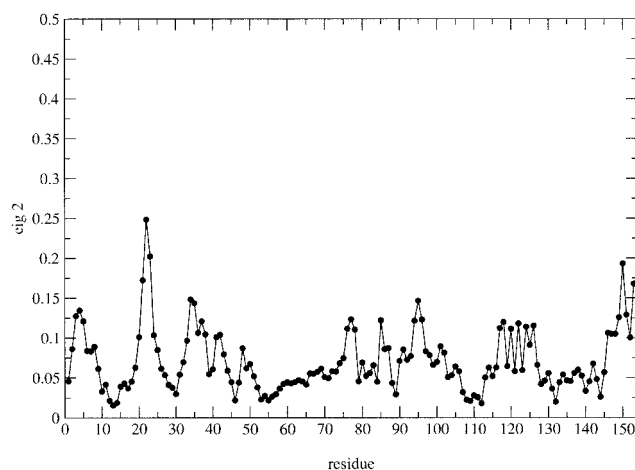


Figure 5. Components of the second C_α eigenvector.

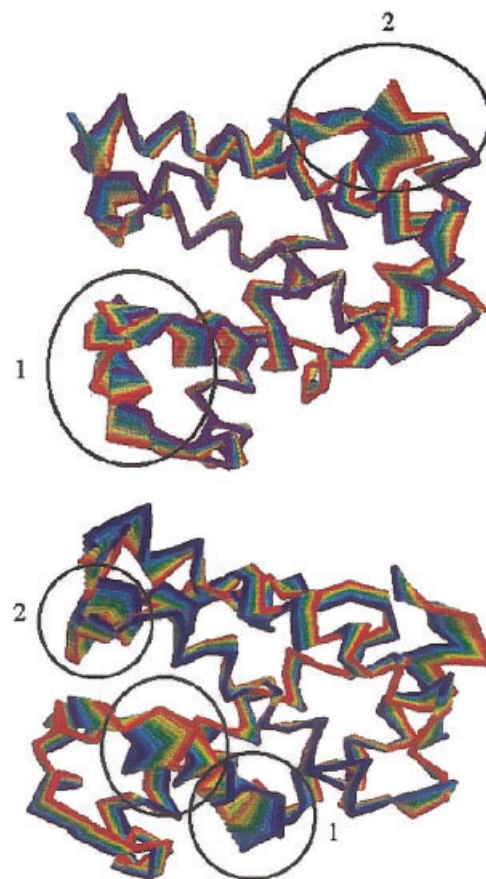


Figure 6. (a) Superposition of 10 configurations obtained from the motion along the first C_α eigenvector. (b) Superposition of ten configurations obtained from the motion along the second C_α eigenvector.

carried out CISD calculations as reported in the Methods section. First of all, we needed to evaluate the accuracy of the employed level of theory. For this purpose we have calculated the ground state of the singlet, triplet, and quintet FeP(Im), and we have compared them with the computational data available in the literature. It should be initially mentioned that the FeP(Im) complex has been widely investigated through several quantum-chemistry methods, in particular based on Density Functional Theory

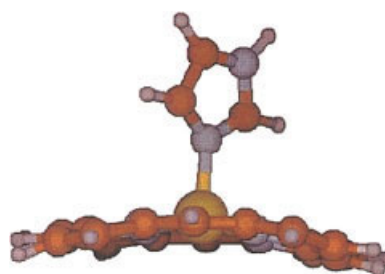


Figure 7. Average structure of the $^5\text{FeP(Im)}$ complex obtained from the MD simulation and used for the quantum chemical calculations.

Table 1. Relative Energies Calculated at CISD Level (Ahlrichs VTZ for Fe^{2+} , STO-3G for C, N, O, H) for the Ground States at Different Spin Multiplicities for the FeP(Im) Complex.

| Spin-state | Energy (eV) | Occupation pattern |
|--------------------|-------------|--|
| $^3\text{FeP(Im)}$ | 0.0 | $d_z^1 d_{xy}^2 d_{xz}^1 d_{yz}^2 d_x^0 d_y^2$ |
| $^1\text{FeP(Im)}$ | 0.9 | $d_z^0 d_{xy}^2 d_{xz}^2 d_{yz}^2 d_x^0 d_y^2$ |
| $^5\text{FeP(Im)}$ | 1.1 | $d_z^1 d_{xy}^1 d_{xz}^2 d_{yz}^1 d_x^2 d_y^2$ |

These calculations were carried out on the average structure from MD simulation.

(DFT).^{32–34} From these calculations it emerged that the ground state of the FeP(Im) *in vacuo* is a triplet state but, the energies of the other magnetic states, i.e., singlet and quintet, are strongly sensitive of the geometry. Of particular importance is the parameter “d,” which essentially defines the deviation of the iron from the plane of the porphyrin ring. The absolute minimum *in vacuo* shows a value of this parameter equal to 0.15 Å and is a triplet. On the other hand, when “d” is shifted to 0.24 Å the ground state becomes a singlet, whereas in correspondence of 0.33 Å the ground state is a quintet. From the crystal structures of deoxy Mb as well as from Infrared, Raman, Electron Spin Resonance, Nuclear Magnetic Resonance, and Mossbauer measurements we know that the experimental value of the parameter “d” is equal to 0.42–0.61 Å, in agreement with the observation of the quintet state as the ground state.^{37,38} Our simulation actually underestimates the value of the parameter “d” with an average value of 0.26 Å. Such a discrepancy is probably to be ascribed to some inaccuracy present in the adopted force field. However, from our calculations, as reported in Table 1, we correctly reproduced, in correspondence of this geometry, the triplet state as the most stable with the singlet and the quintet states lying 0.9 and 1.1 eV higher in energy. Nevertheless, we decided to carry out our investigation on the quintet state, as this is the experimental magnetic condition of deoxy Mb. To evaluate the excited states of the quintet we performed CISD calculations as described in the Methods section. The results concerning the three electronic transitions, i.e., 0–1, 0–2, and 0–3, as well as their related transition moments, are reported in Table 2. In the same table are also reported the corresponding experimental values obtained in aqueous solution, i.e., solvent and protein effects are included. We used such unperturbed basis sets for PMM calculations as described in the following subsection.

PMM Calculations

In the previous two subsections we have described all the computational apparatus, i.e., the electronic characterization of the unperturbed heme and the dynamical characterization of the surrounding protein, necessary for the application of the PMM calculations. We could therefore address the central question of the present investigation: do the large conformational (essential) motions of the protein affect the electronic properties of the quantum center? First of all, we evaluated the reliability of the overall procedure by calculating the electronic spectrum of the deoxy Mb

in solution and comparing our result with the available experimental data. As described in the Theory section, the eigenstates of the quantum center are completely defined by diagonalizing the perturbed Hamiltonian matrix [see eq. (2)]. Within our approximation the perturbation term is provided by the electric field (due to the protein atoms) interacting with the unperturbed dipoles of the quantum center. This is an approximation, which is accurate when the perturbing electric field is essentially constant along the dimension of the complex [see eq. (4)], as indeed found out in our simulation. For each step of the trajectory the perturbing electric field was evaluated in the geometrical center of the FeP(Im) complex using only the protein atomic charges to generate the field. It must be remarked that we neglected the solvent effect, as in our simulations it turned out to hardly modify the main perturbed electronic features of the heme (data not shown), which is essentially buried in the protein. The 9×9 dimensional Hamiltonian matrix was built and diagonalized providing a “trajectory” of perturbed eigenvalues, i.e., the perturbed electronic energies and corresponding eigenvectors. We therefore obtained the ground to the *i*th excited state perturbed energy difference. Obviously, the above electronic energy gaps must be considered as the “vertical” transition energies due to a photon absorption, which is typically the experimentally observable event. At this purpose we have followed, during the trajectory, only the 0–1, 0–2 and 0–3 transitions corresponding to the $d-\pi^*$, Q , and Soret bands reported in Figures 8, 9, and 10. It is interesting to observe, first of all, the different effect of the perturbing field on these three electronic transitions. In fact, for the $d-\pi^*$ transition, with unperturbed excitation energy of 780 nm, we observed a rather marked red-shift oscillating around a value of approximately 826 nm (experimental value about 900 nm). On the other hand, for the other two transitions, the perturbation produced oscillations around almost the unperturbed excitation value. We finally obtained the actual electronic spectrum of deoxy Mb, by simply multiplying the excitation energy distribution with the square length of the corresponding perturbed transition dipoles (see Theory section). We, therefore, compared the maximum of the calculated spectra, reported in Figures 11, 12, and 13 corresponding to 830, 503, and 486 nm for the $d-\pi^*$, Q , and Soret bands, respectively, with the experimental values (900, 560, and 435 nm, respectively). The agreement turned out to be rather good. We could finally address the main point of our investigation. We have just observed, by the width of the electronic spectrum, that the fluctuating environment does affect the eigenstates of the quantum center. Note that in our simulation no quantum vibrations are present, and hence, any vibrational effect is neglected in the model spectra. The energy distribution is due to the protein fluctuations. To further outline and rationalize

Table 2. Vertical Wavelengths for the $^5\text{FeP(Im)}$ Complex in Vacuum, λ^0 , and in Myoglobin in Water, λ_{exp} .⁴⁰

| Transition | Type of transition | λ^0 (nm) | λ_{exp} (nm) |
|------------|-------------------------|------------------|----------------------|
| 0 → 1 | $d \rightarrow \pi^*$ | 780 | ≅900 |
| 0 → 2 | $\pi \rightarrow \pi^*$ | 497 | 560 |
| 0 → 3 | $\pi \rightarrow \pi^*$ | 487 | 435 |

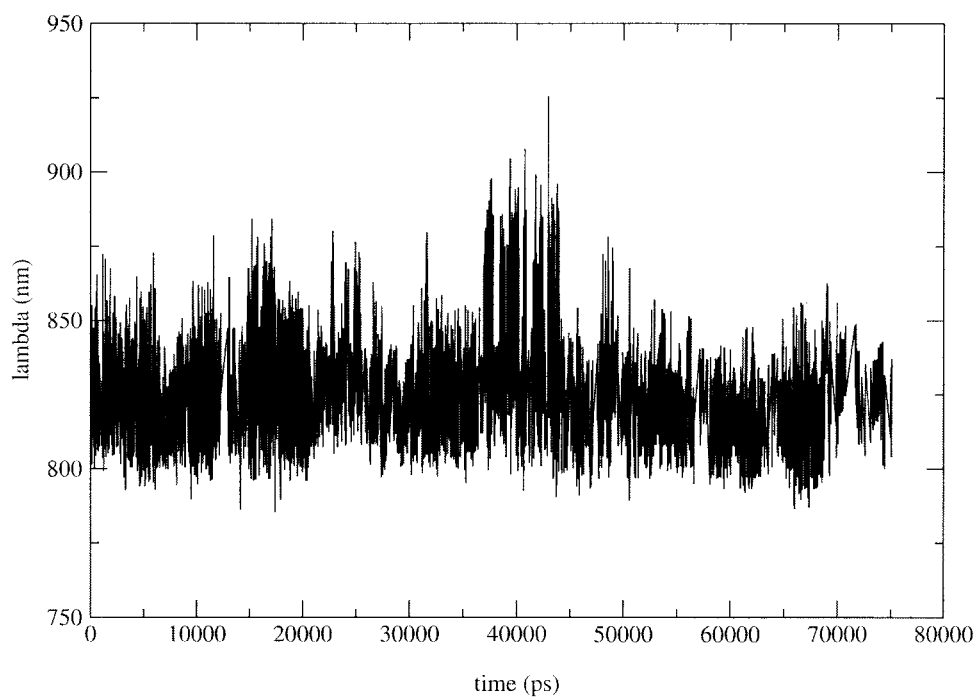


Figure 8. Time course for the 0–1 excitation energy as obtained by PMM calculation during the MD simulation.

such a result we have, however, readdressed the question in terms of correlation between the essential motions of the deoxy Mb and the heme electronic properties. As already remarked we focused

only on the first two essential eigenvectors that account for a large part of the C-alpha motion. In Figure 14, we have reported the average $d-\pi^*$ transition energy as a function of the position along

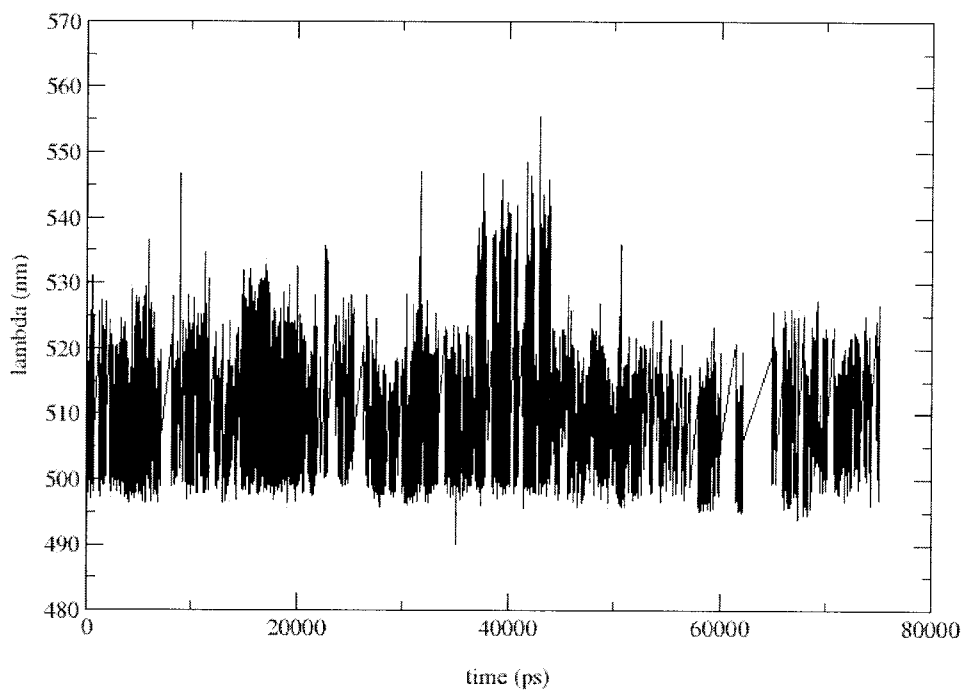


Figure 9. Time course for the 0–2 excitation energy as obtained by PMM calculation during the MD simulation.

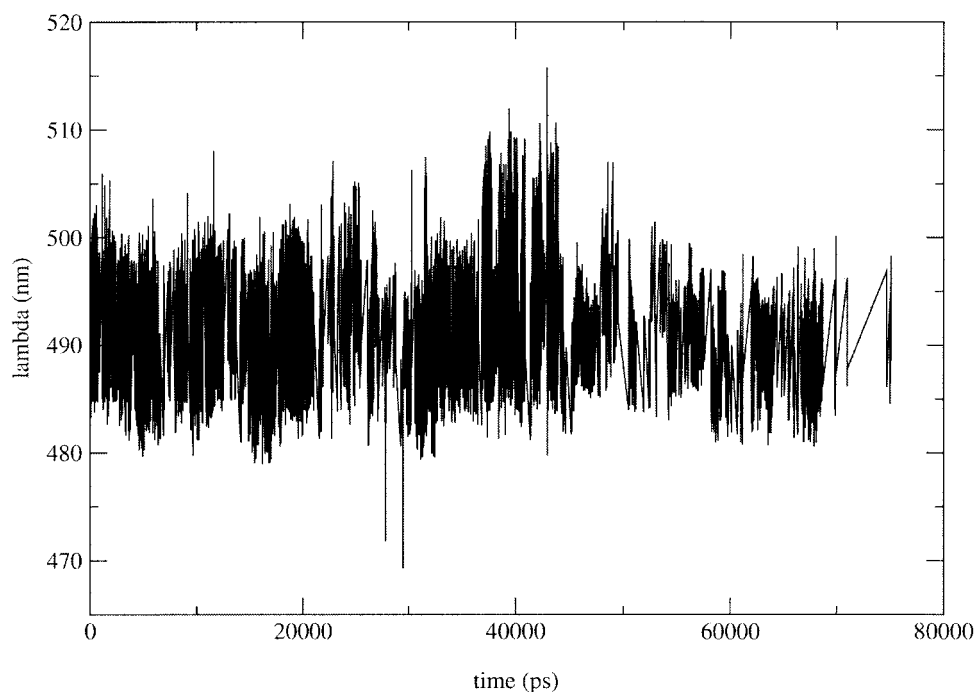


Figure 10. Time course for the 0–3 excitation energy as obtained by PMM calculation during the MD simulation.

the first eigenvector. In Figure 15 we also reported the corresponding standard deviation. From these figures it could be observed that the first essential degree of freedom of the deoxy Mb sharply alters this vertical excitation wavelength which, consequently, turned out to span a region as large as 20 nm with a well defined minimum value. The error bars resulted to be rather small but, at the same time, the fluctuations around the average values, shown in Figure 15, turned out to be much more quantitatively important and dependent on the conformational coordinate. These results clearly show that large concerted motions of the deoxy Mb significantly

alter the ground to first excited state energy gap. To inspect the role of the second eigenvector we have also reported, in Figure 16, the average 0–1 energy gap as a function of the position in the plane defined by the first two essential motions (eigenvectors). The resulting surface again shows a clear coupling between these two conformational motions and the excitation energy. Moreover, according to eq. (14), we also evaluated the excitation Helmholtz free energy. In Figures 17 and 18, the excitation Helmholtz free energy is plotted as a function of the position along the first eigenvector as well as in the plane of the first two eigenvectors. It

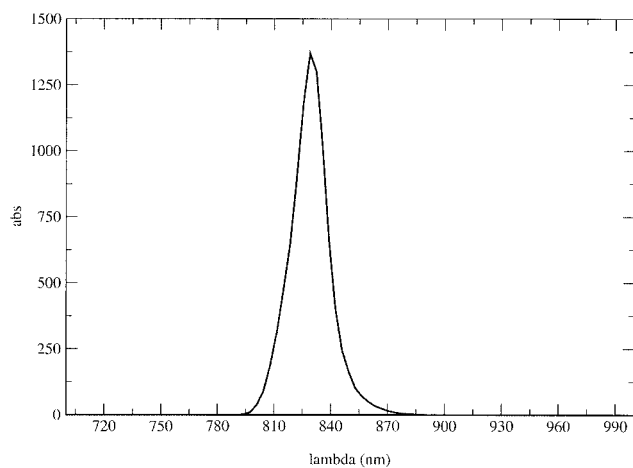


Figure 11. Spectral profile for the 0–1 transition.

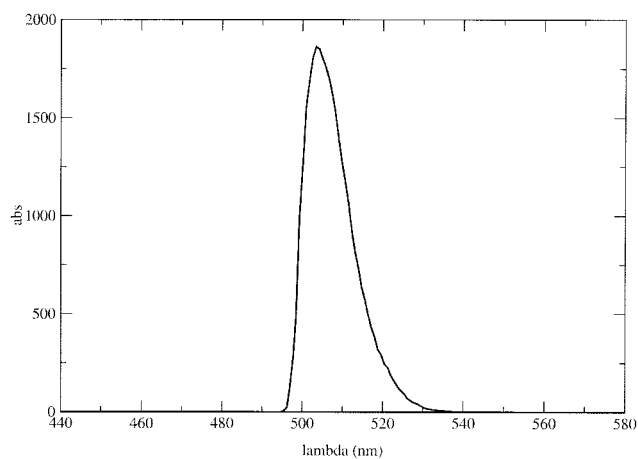


Figure 12. Spectral profile for the 0–2 transition.

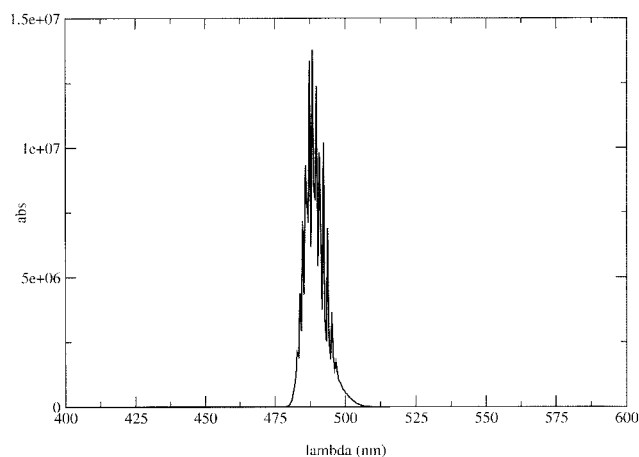


Figure 13. Spectral profile for the 0–3 transition.

is evident that thermal excitation is not a spontaneous process but, at the same time, there is a region of the first eigenvector, i.e., the central part, where the free energy reaches a well-defined minimum and the probability of excitation undergoes a slight increase. Finally, we have carried out a detailed investigation on the actual nature of the perturbing field. As for the atomic fluctuations, we have performed an essential dynamics analysis of the fluctuating electric field on the heme geometrical center. For this purpose, a covariance matrix was built using the components of the electric field generated by each residue of deoxy Mb. Hence, by diagonalizing this covariance matrix we obtain the set of eigenvectors and eigenvalues that characterize the complex fluctuations of the electric field. In Figure 19 we report the corresponding cumulative fluctuations. Not surprisingly, the first 10 eigenvectors basically account for more than 75% of the overall electric field fluctuation. Analyzing in more details the nature of the first two eigenvectors, shown in Figures 20 and 21, it emerged that basically three

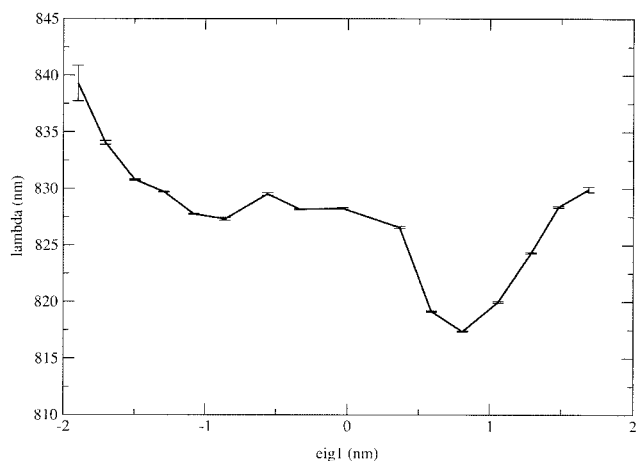


Figure 14. Average excitation wavelength for the 0–1 transition as a function of the position along the first C_α eigenvector. In the figure the error bars are also shown.

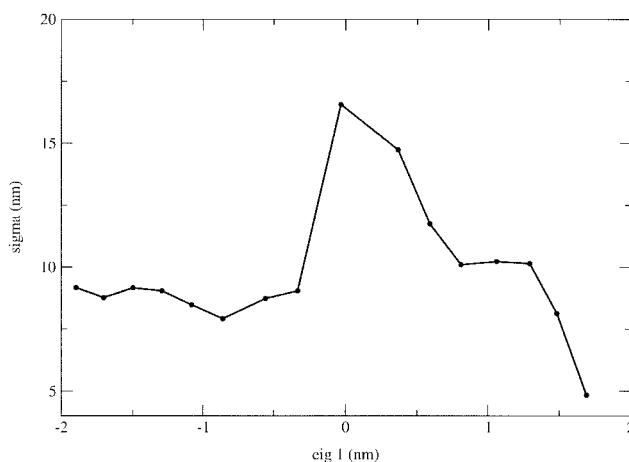


Figure 15. Standard deviation of the excitation wavelength for the 0–1 transition as a function of the position along the first C_α eigenvector.

residues, i.e., Hys97, Lys96, and, to a minor extent the distal His64 mainly contribute to the electric field fluctuations. In other words, these three residues can be considered, as the main source for the perturbation on the quantum center, and hence, of the fluctuations of the excitation energy. Interestingly, the analysis of the amino acid sequence revealed that beyond the obvious conservation of the distal histidine (His 64) involved in the oxygen binding to the heme, Hys97 and Lys96 are also rather well conserved in the primary sequence of many myoglobins.³⁹

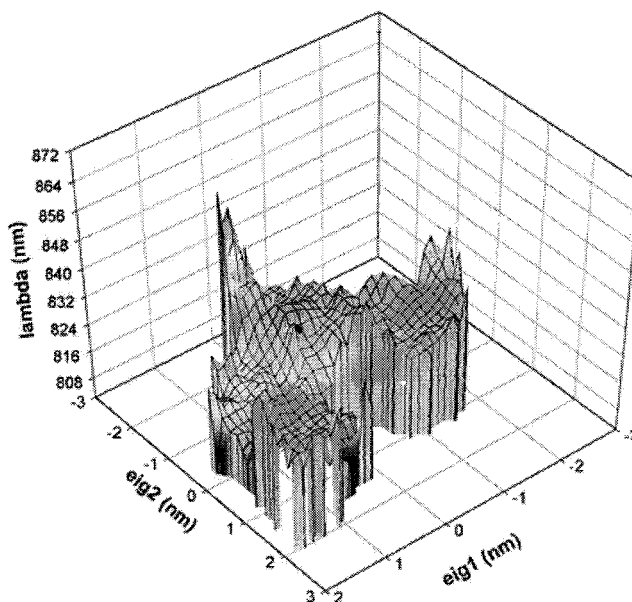


Figure 16. Average excitation wavelength for the 0–1 transition as a function of the position along the first two C_α eigenvectors.

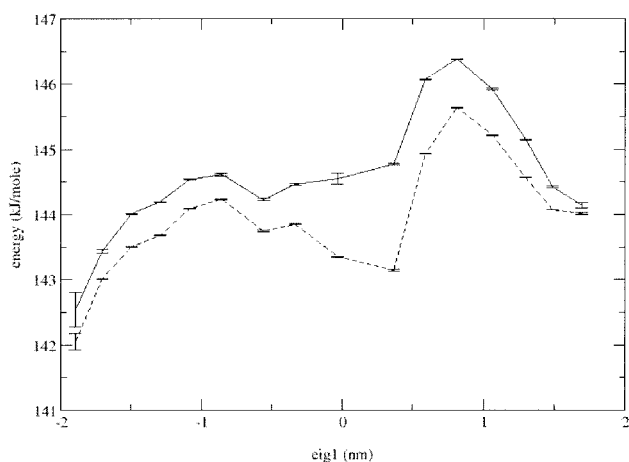


Figure 17. Excitation energy (solid line) and free energy (dashed line) for the 0–1 transition as a function of the position along the first C_{α} eigenvector. In the figure, the error bars are also shown.

Conclusions

In this article we used a long MD simulation (80 ns) in combination with PMM calculations, to investigate the influence of conformational fluctuations on the electronic properties of the heme in Myoglobin. Results showed a clear coupling between the main collective internal motions of Myoglobin and the electronic properties of heme (heme molecular orbitals), confirming previous results on a protein involved in photosynthesis.¹³ Such a coupling support the idea that proteins conformational behavior may modulate the electronic levels that are important in the transition states of the chemical reactions occurring inside the protein. Hence, these

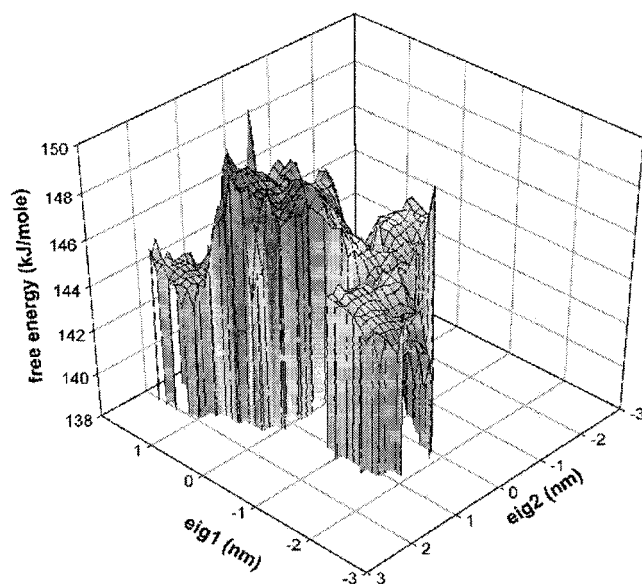


Figure 18. Excitation free energy for the 0–1 transition as a function of the position along the first two C_{α} eigenvectors.

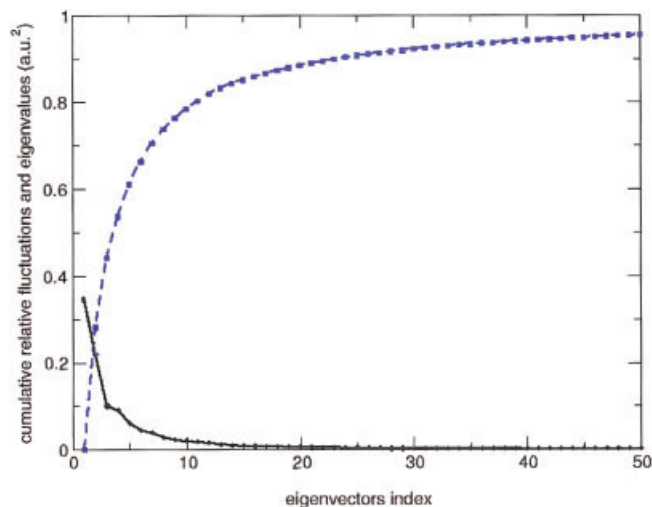


Figure 19. Normalized eigenvalues (circles) and cumulative fluctuations (squares) for the electric field generated by each residue. [Color figure can be viewed in the online issue, which is available at <http://www.interscience.wiley.com>]

results suggest a possible conformational regulation mechanism for ligand binding to heme, based on the perturbation of the reaction transition state. Moreover, the analysis of the electric field fluctuations pointed out a few residues as key residues in modulating heme electronic properties and, interestingly, such residues are largely conserved in higher species. Finally, the comparison of our calculated spectra with experimental ones indicated that PMM approach can be reliable also in these large and complex systems. Such results make the proposed procedure very promising for the study of chromophores and chemical reactions in complex systems where it is expected a relevant coupling between the electronic behavior and molecular motions. In particular, for biochemical systems, PMM approach could be important for understanding the complex effects of conformational fluctuations and chemical co-factors in enzymatic reactions.

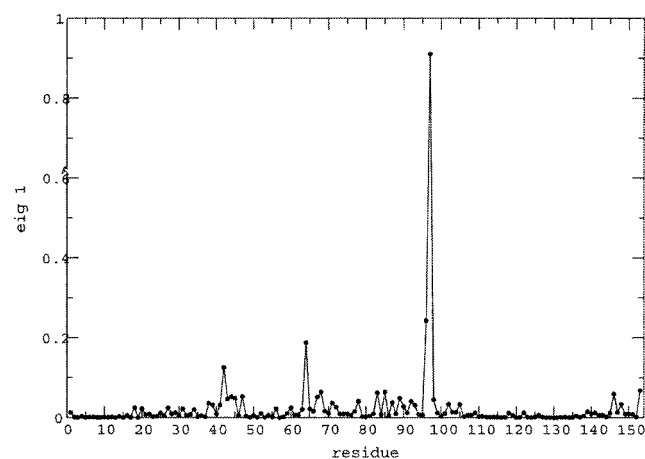


Figure 20. Components of the first electric field eigenvector.

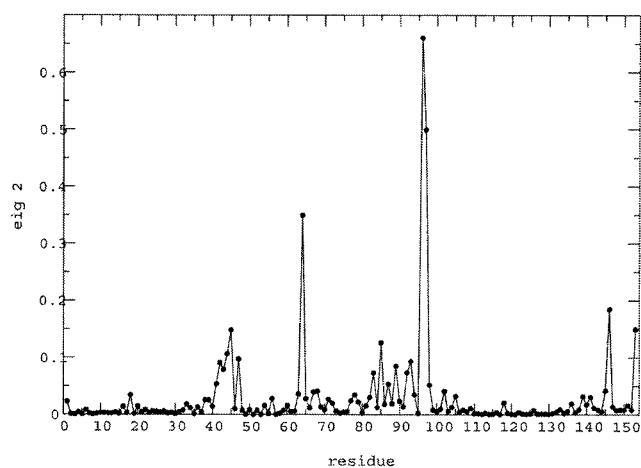


Figure 21. Components of the second electric field eigenvector.

Acknowledgments

We acknowledge Prof. M. Brunori for information and stimulating discussions on Myoglobin, and the Supercomputing Center for University and Research (CASPUR-Rome) for some of the computational facilities.

References

- Smith, J.; Kuczera, K.; Karplus, M. *Proc Natl Acad Sci USA* 1990, 87, 1601.
- van Aalten, D. M. F.; Amadei, A.; Vriend, G.; Linssen, A. B. M.; Eijssink, V. G. H.; Vriend, G.; Berendsen, H. J. C. *Proteins Struct Funct Genet* 1995, 22, 45.
- Chillemi, G.; Falconi, M.; Amadei, A.; Zimatore, G.; Desideri, A.; Di Nola, A. *Biophys J* 1997, 73, 1007.
- Duan, Y.; Kollman, P. *Science* 1998, 282, 740.
- de Groot, B. L.; Grubmüller, H. *Science* 2001, 294, 2353.
- Friesner, R. A.; Dunietz, B. D. *Acc Chem Res* 2001, 34, 351.
- Gerber, R. B.; Jungwirth, P. *Chem Rev* 1999, 99, 1583.
- Defranceschi, M.; Bris, C. L. *Int J Quantum Chem* 1999, 71, 227.
- Kollman, P.; Kuhn, B.; Donini, O.; Perakyla, M.; Stanton, R.; Bakowies, D. *Acc Chem Res* 2001, 34, 72.
- Piana, S.; Carloni, P.; Parrinello, M. *J Mol Biol* 2002, 319, 567.
- Aschi, M.; Spezia, R.; Di Nola, A.; Amadei, A. *Chem Phys Lett* 2001, 344, 374.
- Spezia, R.; Aschi, M.; Di Nola, A.; Amadei, A. *Chem Phys Lett* 2002, 365, 450.
- Spezia, R.; Aschi, M.; Di Nola, A.; Valentin, M. D.; Carbonera, D.; Amadei, A. *Biophys J* 2003, 84, 2805.
- Straub, J. E.; Karplus, M. *Chem Phys* 1991, 158, 221.
- Kuczera, K.; Lambry, J.; Martin, J.; Karplus, M. *Proc Natl Acad Sci USA* 1993, 90, 5805.
- Hill, J. R.; Tokmakoff, A.; Peterson, K. A.; Sauter, B.; Zimdars, D.; Dlott, D. D.; Fayer, M. D. *J Phys Chem* 1994, 98, 11213.
- Springer, B. A.; Sligar, S. G.; Olson, J. S.; Phillips, G. N. *J. Chem Rev* 1994, 94, 699.
- Shikama, K. *Chem Rev* 1998, 98, 1357.
- Merchant, K. A.; Thompson, D. E.; Xu, Q. H.; Williams, R. B.; Fayer, M. D. *Biophys J* 2002, 82, 3277.
- Eaton, W. A.; Hanson, L. K.; Stephens, P. J.; J. C. Sutherland, J. B. R. D. *J Am Chem Soc* 1978, 100, 4991.
- Sono, M.; Andersson, L. A.; Dawson, J. H. *J Biol Chem* 1982, 257, 8308.
- Popov, A. N.; Kachalova, G. S.; Bartunik, H. D. *Science* 1999, 284, 473.
- Berendsen, H. J. C.; Postma, J. P. M.; van Gunsteren, W. F.; Hermans, J. In *Intermolecular Forces*; Pullman, B., Ed.; Reidel: Dordrecht, 1981.
- Evans, D. J.; Morriss, G. P. *Statistical Mechanics of Nonequilibrium Liquids*; Academic Press: London, 1990.
- Darden, T. A.; York, D. M.; Pedersen, L. G. *J Chem Phys* 1993, 98, 10089.
- Hess, B.; Bekker, H.; Berendsen, H. J. C.; Fraaije, J. G. E. M. *J Comput Chem* 1997, 18, 1463.
- Amadei, A.; Chillemi, G.; Ceruso, M. A.; Grottesi, A.; Di Nola, A. *J Chem Phys* 2000, 112, 9.
- Berendsen, H. J. C.; Postma, J. P. M.; van Gunsteren, W. F.; Hermans, J. In *Intermolecular Forces*; Pullmann, B., Ed.; D. Reider Publishing Company: Dordrecht, 1981, p. 331.
- Foresman, J. B.; Head-Gordon, M.; Pople, J. A.; Frisch, M. J. *J Phys Chem* 1992, 96, 135.
- Schafer, A.; Horn, H.; Ahlrichs, R. *J Chem Phys* 1992, 97, 2571.
- Hehre, W. J.; Stewart, R. F.; Pople, J. A. *J Chem Phys* 1969, 2657.
- Kozłowski, P. M.; Spiro, T. G.; Zgierski, M. Z. *J Phys Chem B* 2000, 104, 10659.
- Rovira, C.; Ballone, P.; Parrinello, M. *Chem Phys Lett* 1997, 271, 247.
- Kozłowski, P. M.; Spiro, T. G. *J Phys Chem B* 1998, 102, 2603.
- Schmidt, M. W.; Baldrige, K. K.; Boatz, J. A.; Elbert, S. T.; Gordon, M. S.; Jensen, J. J.; Koseki, S.; Matsunaga, N.; Nguyen, K. A.; Su, S.; Windus, T. L.; Dupuis, M.; Montgomery, J. A. *J Comput Chem* 1993, 14, 1347.
- Amadei, A.; Linssen, A. B. M.; Berendsen, H. J. C. *Proteins Struct Funct Genet* 1993, 17, 412.
- Momenteau, M.; Reed, C. A. *Chem Rev* 1994, 94, 659.
- Bougault, C. M.; Dou, Y.; Ikeda-Saito, M.; Langry, K. C.; Smith, K. M.; Mar, G. N. L. *J Am Chem Soc* 1998, 120, 2113.
- Phillips, G. N. *Handbook of Metalloproteins*; John Wiley and Sons, Inc.: New York, 1990.
- Lim, M.; Jackson, T. A.; Anfirud, P. A. *J Phys Chem* 1996, 100, 12043.